



**HAL**  
open science

## Impact of Oxygen on Corrosion and Hydrogen Permeation of Pure iron in the Presence of H<sub>2</sub>S

J. Kittel, N. Ferrando, Martien Duvall Deffo Ayagou, Christophe Mendibide, Eliane Sutter, Thi Tuyet Mai Tran, Bernard Tribollet

► **To cite this version:**

J. Kittel, N. Ferrando, Martien Duvall Deffo Ayagou, Christophe Mendibide, Eliane Sutter, et al.. Impact of Oxygen on Corrosion and Hydrogen Permeation of Pure iron in the Presence of H<sub>2</sub>S. Eurocorr 2017, Sep 2017, Praha, Czech Republic. hal-02462631

**HAL Id: hal-02462631**

**<https://ifp.hal.science/hal-02462631>**

Submitted on 31 Jan 2020

**HAL** is a multi-disciplinary open access archive for the deposit and dissemination of scientific research documents, whether they are published or not. The documents may come from teaching and research institutions in France or abroad, or from public or private research centers.

L'archive ouverte pluridisciplinaire **HAL**, est destinée au dépôt et à la diffusion de documents scientifiques de niveau recherche, publiés ou non, émanant des établissements d'enseignement et de recherche français ou étrangers, des laboratoires publics ou privés.

# Impact of Oxygen on Corrosion and Hydrogen Permeation of Pure iron in the Presence of H<sub>2</sub>S

Martien Duvall Deffo-Ayagou, Christophe Mendibide, Claude Duret-Thual, Institut de la Corrosion – Site de Saint-Etienne, Zone d'activités du Parc secteur Gampille, 42490 Fraisses, France

Eliane Sutter, Mai Tran, Bernard Tribollet, Laboratoire Interfaces et Systèmes Electrochimiques (LISE), UPR 15 du CNRS, 75252 Paris Cedex 05

N. Ferrando, J. Kittel, IFP Energies nouvelles, Rond-Point de l'échangeur de Solaize BP3, 69360 Solaize, France

## Abstract

This paper examines the influence of oxygen traces on corrosion and hydrogen charging of steel in H<sub>2</sub>S containing environment. It is well known that H<sub>2</sub>S is the driving force for many types of steel failures such as hydrogen induced cracking (HIC), sulfide stress cracking (SSC), and stress-oriented hydrogen induced cracking (SOHIC). Since it is a huge concern for oil and gas industries, standard test methods have been developed and published as NACE technical methods (e.g. NACE TM0284 and NACE TM0177). Though it is recognized that oxygen pollution shall be avoided during H<sub>2</sub>S cracking tests, there is still a lack of experimental data to illustrate the potential impacts of a small oxygen pollution.

The aim of the present study was to check if oxygen traces can modify corrosion mechanisms and hydrogen charging of steel in H<sub>2</sub>S medium. Experiments consisted in hydrogen permeation measurements through thin pure iron membrane. They were performed at corrosion potential in order to be in realistic environmental conditions. Corrosion rate was also evaluated through weight loss measurements. Analysis of test solutions was performed in order to identify reaction products between H<sub>2</sub>S and O<sub>2</sub>.

## 1 Introduction

Materials used in oil and gas industries are exposed to sour environments containing hydrogen sulfide (H<sub>2</sub>S), which is corrosive and known to promote hydrogen entry in steels. This may lead to several types of steel failures such as HIC, SSC, and SOHIC.

Corrosion and hydrogen embrittlement of steels in H<sub>2</sub>S containing environments has been studied for several decades. Standard tests have been developed in the seventies and eighties by the European Federation of Corrosion and by the NACE, for the selection and the

qualification of steels for use in H<sub>2</sub>S containing environments, e.g. NACE TM 0177 for SSC testing, and NACE TM0284 for HIC testing [1]. These standards strongly recommend to avoid oxygen infiltration in test environments in order to represent real field conditions. However, they do not give any information on the effects of oxygen on the test results. There are many different ways by which oxygen can pollute a test medium such as, a poor deaeration of the initial test solution, poor sealing of test reactors, the use of piping permeable to oxygen, and diverse other operations during the test (solution sampling, pH adjustment, etc.). Therefore, it is important to study and understand the effects of oxygen traces on corrosion and hydrogen charging of steel in H<sub>2</sub>S containing environment.

It has been shown by Song *et al.*, that a solution continuously bubbled with a mixture of H<sub>2</sub>S and O<sub>2</sub>, acidifies continuously and does not rise back to neutrality after H<sub>2</sub>S purging with inert gas (argon, nitrogen) [2]. This experimental finding is in good agreement with the reaction pathway proposed by Crolet and Pourbaix, showing that O<sub>2</sub> – H<sub>2</sub>S can react to form thiosulfate or tetrathionate [3]. In both cases, H<sup>+</sup> is also produced, resulting in a decrease of pH. The produced S-O compounds can then modify the kinetics and corrosion mechanisms.

It is also well-known that H<sub>2</sub>S promotes hydrogen entry in steels via sulfurs adsorbates which can interact with oxygen adsorbates in the case of any oxygen pollution [4–6]. Oxygen traces in H<sub>2</sub>S containing environment could then:

- Modify the corrosive environment by reacting with H<sub>2</sub>S
- Modify the corrosion rate and corrosion deposits
- And modify the hydrogen entry in steels

This paper aims to improve the understanding of corrosion mechanisms and hydrogen charging of steels in H<sub>2</sub>S containing environment polluted with oxygen traces. Typical experiments consisted in exposing iron coupons in water saturated with H<sub>2</sub>S and with a continuous and well controlled O<sub>2</sub> entry. Chemical analysis of the test solution was performed in order to identify reaction products between O<sub>2</sub> and H<sub>2</sub>S. Electrochemical measurements were also carried out to evaluate the effect of O<sub>2</sub> on corrosion and on hydrogen entry in the metal.

## **2 Experimental procedure**

### **2.1 Control of oxygen in test media**

In order to control the quantity of oxygen introduced in the test cell, we used two mass flowmeters. The first one controls H<sub>2</sub>S flow rate (0 to 20 mL/min) and the second one controls

O<sub>2</sub>/N<sub>2</sub> mixture flowrate (0 to 3 mL/min). Gas lines are made of 316L stainless steel and several valves are used to manage the gas supply into the cell. Gases are homogenized in a spiral gas line of about 1 meter before bubbling into the test solution and the oxygen content in the gas line immediately before entering into the test cell is checked with a HACH 410 Orbisphere probe as shown in Figure 1.

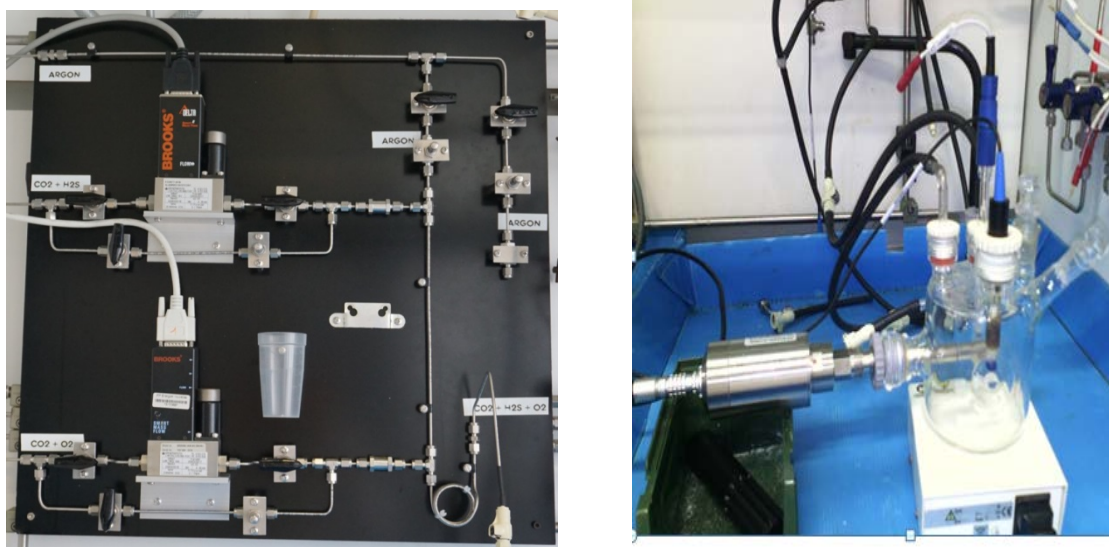


**Figure 1 : Oxygen control experimental set up**

## **2.2 Corrosive medium**

The support electrolyte contained NaCl (35g/L). In order to avoid side effects of other chemicals, no additional buffer (bicarbonates, acetates, etc.) was added, so that pH could evolve freely during the test. Continuous bubbling of gases was maintained during all experiments. Two gas compositions were tested: pure H<sub>2</sub>S and a mixture of H<sub>2</sub>S (87.5%), N<sub>2</sub> (11.25%) and O<sub>2</sub> (1.25%) corresponding to 500 mass. ppb dissolved O<sub>2</sub> according to Henry's law.

## **2.3 Permeation set-up**

Permeation measurements were performed using the electrochemical technique with a Devanathan-Stachurski type cell [7]. The experimental setup was made of twin cells separated by the steel membrane as shown in Figure 2. They were equipped with double jacket in order to maintain the temperature at 24°C +/- 2°C.

The membrane consisted in pure iron, with the exit face covered by palladium following well established procedures [8]. Membrane thickness was 0.5 mm. With such thickness and in H<sub>2</sub>S environment, it is considered that permeation is mostly governed by reactions at the entry face, minimizing the impact of bulk diffusion of hydrogen.

As for the literature in regards to hydrogen charging in an H<sub>2</sub>S environment, the charging face of the membrane was maintained at the corrosion potential, though it is known that permeation transients are often strongly affected by the very fast precipitation of a FeS layer, which may hinder the potential impact of O<sub>2</sub>/H<sub>2</sub>S ratio. Therefore, at the beginning of each experiment, the charging side of the membrane was left at free potential. This procedure has the advantage of being representative of exposure conditions in standard tests for HIC or SSC.

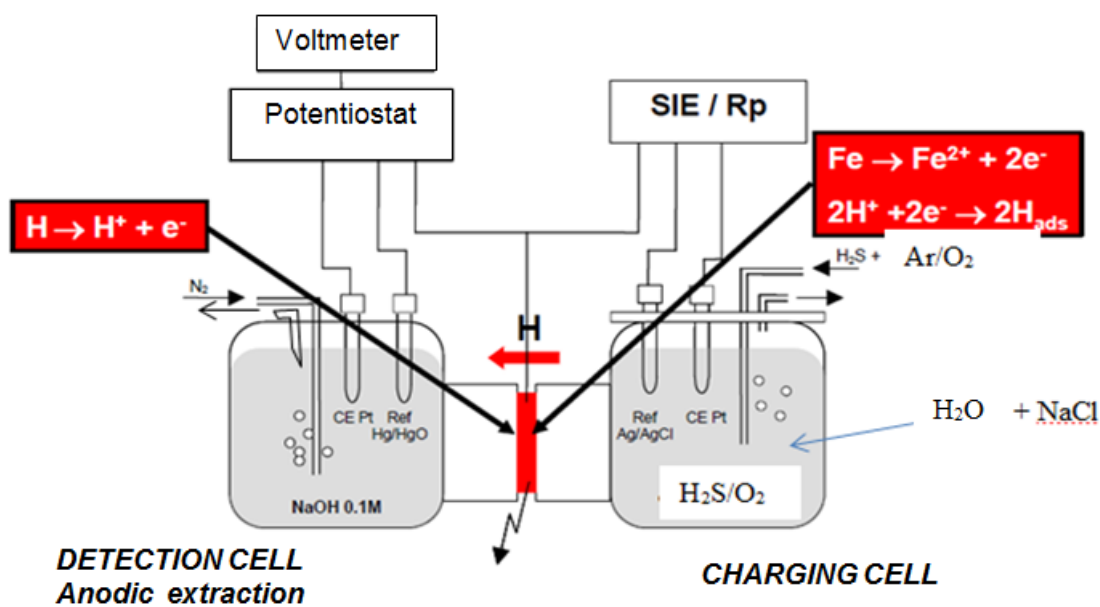


**Figure 2 : Permeation set up**

The exit surface of the membrane was held in a deoxygenated 0.1 mol.L<sup>-1</sup> NaOH solution and polarized at an anodic potential of 250 mV vs. Hg/HgO (1M KOH) reference electrode providing a direct measurement of the hydrogen flux across the steel membrane.

In addition to the permeation membrane, weight-loss specimens (0.9 cm x 0.9 cm x 0.05 cm) were also introduced into the charging cell. These coupons were used for weight-loss corrosion rate evaluation, as well as surface analysis by Scanning Electronic Microscopy (SEM), and X-Ray Diffraction (XRD).

During each test, the charging solution was periodically sampled and analyzed by ionic chromatography (IC) to determine the sulfur–oxygen (S-O) species concentrations. At the end of the test, the total sulfur content in the charging solution was analyzed by Inductively Coupled Plasma Emission Spectroscopy (ICPES).

## 2.4 Tested material

The material used for the permeation tests is a pure iron disc (99.5%) of 57 mm diameter and thickness 0.5 mm with a tongue of 7 \* 7 mm for the electrical connection. The disc was heat treated under vacuum at 900° C for 30 minutes. The chemical composition of the disc is shown in Table 1. Pure iron is used as a model material to avoid as much as possible a contribution of microstructural defects in permeation results.

Table 1 : Chemical composition of test material

Element	Al	Cr	Cu	Mn	Ni	Si	Ti	C	P	S	Fe
Content (mass. ppm)	107	133	55	240	159	100	5	18	60	48	Bal.

## 3 Results

### 3.1 Calibration and measurement of oxygen concentration within the cell

Verification of the gas mixing system was performed using CO<sub>2</sub> as acid gas instead of H<sub>2</sub>S. Different levels of O<sub>2</sub> were then obtained by selecting different flow rates for both gas lines. The results are illustrated in Figure 3. The dissolved oxygen content of the test solution is related to the oxygen partial pressure in the gas phase. Indeed, the dissolved oxygen content follows Henry's law, which shows a linear dependence between the concentration of a dissolved gas in a given solution and its content in the gas phase in equilibrium. According to Henry's law:

$$C_i = K_{Hi} P_i$$

*C<sub>i</sub>* = dissolved gas concentration, *K<sub>Hi</sub>* = Henry's constant of gaz *i*, and *P<sub>i</sub>* = gas partial pressure.

The Henry's constant values for H<sub>2</sub>S and O<sub>2</sub> at 25°C and 1 atm are respectively 0.1 mol/L/bar and 1.3 x 10<sup>-3</sup> mol/L/bar [3,7,9,10]. The corresponding oxygen partial pressures for targeted dissolved oxygen content are presented in Table 2. Theoretical and experimental values for dissolved oxygen content are observed to be really close, it can then be assumed that the test conditions are close to ideality, and Henry's law is therefore applicable.

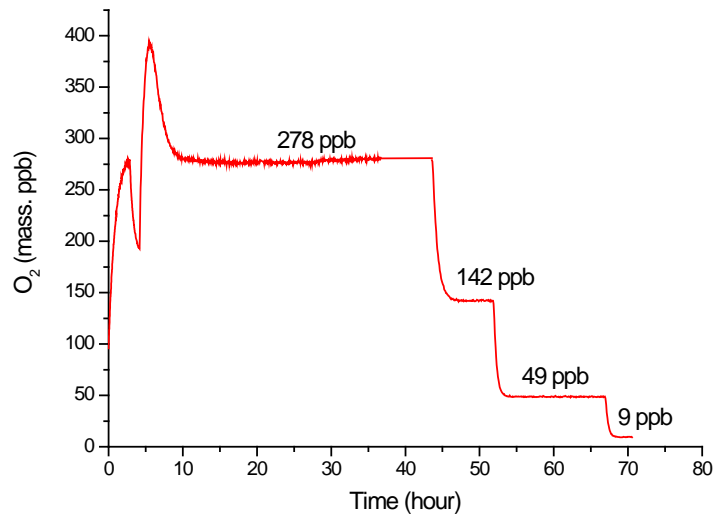


Figure 3 : Control of oxygen content in the test medium

Table 2 : Oxygen partial pressure for targeted dissolved oxygen content

Target O <sub>2</sub> partial pressure (mbar)	Theoretical dissolved oxygen content (ppb)	Experimental dissolved oxygen content (ppb)
7	290	278
3.6	150	142
1.2	50	49
0.24	10	9

It could be concluded from these tests that our gas mixing system allowed to control oxygen content at least up to 12 mbar, corresponding to approximately 500 ppb dissolved O<sub>2</sub>.

### 3.2 Impact of oxygen on corrosive medium

The pH trends of test solutions without or with oxygen (500 ppb) are shown in Figure 4. These pH measurements were performed during a permeation experiment, i.e. with iron coupons in the test solution. In the beginning of both tests, pH is close to 3.9, corresponding to H<sub>2</sub>S saturated water at 1 bar. As expected, pH then increases up to 4.3, corresponding to FeS saturation. Once saturation is reached, no change of pH is observed for the test without O<sub>2</sub>. On the contrary the test solution treated with both H<sub>2</sub>S and O<sub>2</sub> shows a continuous decrease of pH until the end of the test. After 1 month exposure, the pH has decreased by more than 1 unit.

Thus at the end of the test, the oxygen free solution has a pH value of 4.4 and the solution treated with both H<sub>2</sub>S and O<sub>2</sub> has a pH value of 3.2.

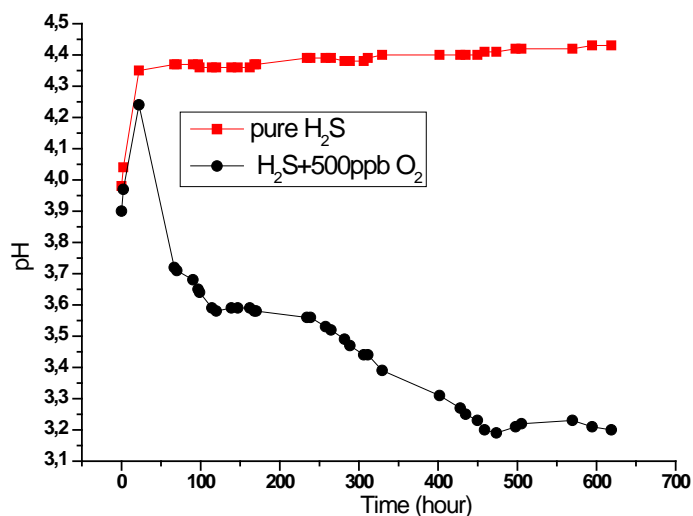
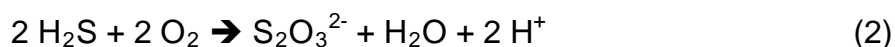


Figure 4 : pH trend of tests solutions

The figure shows that during the first hours of the test in both solutions, the major reaction is the corrosion of iron which produces alkalinity and dissolved iron and consequently increases the pH. Once iron sulfide saturation is reached, the pH stops increasing. In the solution treated with oxygen, there are additional reactions between oxygen and H<sub>2</sub>S producing S-O species which acidify the medium in agreement with Song and Crolet works [2,3] as shown in equations (1-3). Over a long period this cumulative acidification can have a considerable effect on the pH of the solution.



In addition to in situ pH measurements, periodic sampling of the test solutions was performed for chemical analysis. The main findings are plotted on Figure 5. Before analysis by ionic chromatography, residual dissolved H<sub>2</sub>S was eliminated by argon stripping in the water aliquot. The main dissolved sulfur compound detected was sulfate.

In the solution treated with oxygen, the sulfate concentrations increases gradually until the end of the test. In the same condition, we also observed a white elemental sulfur deposit in the cell. Sulfites and thiosulfates were also detected at trace levels. These results are compatibles with

research carried out by Crolet and Song [2,3]. According to their research, thiosulfate is expected to form, however it is known that thiosulfate is unstable and is oxidized to sulfate and elemental sulfur in oxygen containing environment.

On the contrary, tests conducted without added oxygen did not show any elemental sulfur precipitation and no significant increase of sulfate, sulfite or thiosulfate content.

ICPES results showed that solution treated with oxygen contained of 45 ppm of total sulfur. Hence, sulfur compound detected by ionic chromatography represent around 70% of dissolved sulfur.

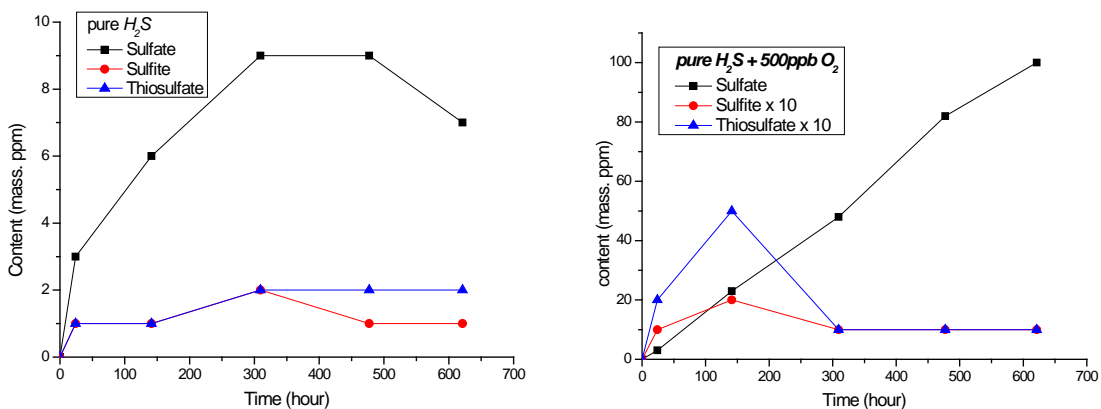


Figure 5 : S-O content in test media

### 3.3 Impact of oxygen on corrosion rate and corrosion products

The results showing the effect of oxygen on corrosion rate are presented in Figure 6. Four series of tests were performed in parallel, with and without oxygen. As expected, oxygen pollution results in a strong increase of corrosion rate, by a factor of 2, compared to experiment carried out without oxygen. This increase in corrosion rate can be interpreted as an effect of the decrease in pH. It is also possible that oxygen contributes directly to the cathodic current density and then increases the corrosion rate.

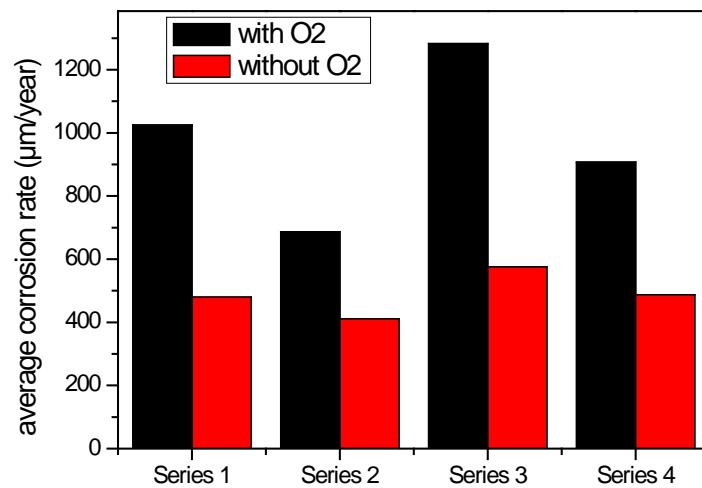


Figure 6 : Comparisons of corrosion rates for several tests with and without oxygen pollution

Some differences on corrosion products during test with and without oxygen were also observed as shown in Figure 7. The SEM observation shows for the oxygen-free tests a rather homogeneous surface and the Electron-Dispersive Spectroscopy (EDS) cartography shows almost uniform surface coverage by sulfur. On the other hand for the test in the presence of oxygen, the EDS cartography shows differences in the deposits with zones rich in oxygen and others rich in sulfur. The characterization by XRD shows that in both cases the deposits consist essentially of mackinawite and greigite, but in the tests carried out in the presence of oxygen, it is observed, in addition, large deposits of elemental sulfur and marcasite.

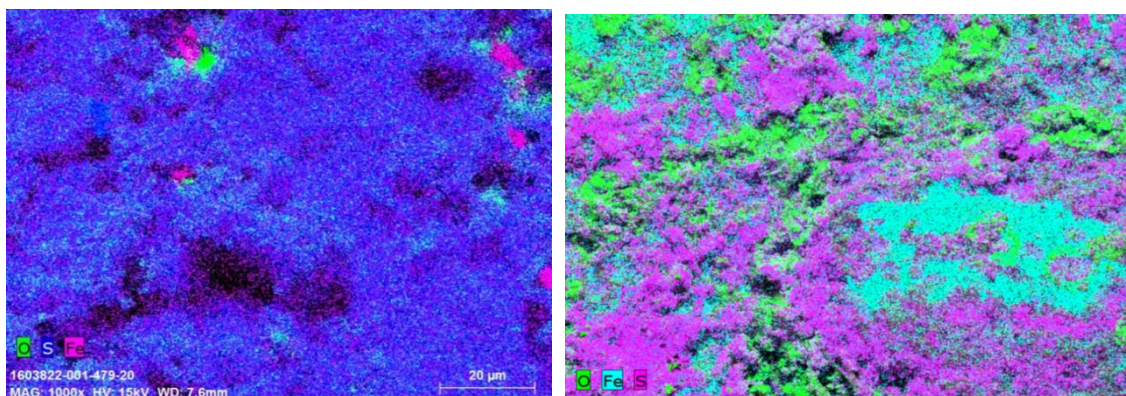


Figure 7 : EDS image for corrosion products a) without oxygen b) with oxygen

### 3.4 Impact of oxygen on hydrogen permeation

The effects of oxygen on permeation through a pure iron membrane in NaCl saturated solution with 1 bar H<sub>2</sub>S are illustrated in Figure 8. No particular effect of oxygen is observed on the permeation current during the first hundred hours of the test. However, after 200 h, a linear decrease in the hydrogen permeation current is observed in the presence of O<sub>2</sub>. After 25 days of tests, the permeation current density was about 39 and 19  $\mu\text{A}/\text{cm}^2$  respectively in the solution without oxygen and in the solution treated with oxygen. This trend is reproducible for the four sets of tests that have been done under these conditions.

This decrease of permeation current is somewhat unexpected, since it was observed that in oxygen treated solution, the pH decreases with time down to 3.2, while it stayed close to 4.4 without O<sub>2</sub> pollution. Therefore it was expected to observe an increase in permeation current density in the presence of oxygen since it has been shown that hydrogen flux is enhanced as pH decreases [11].

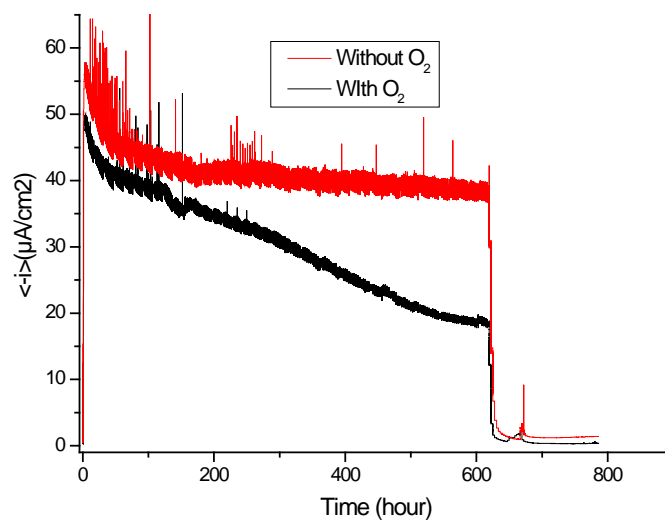


Figure 8 : Permeation curves in H<sub>2</sub>S medium with or without oxygen.

The decreasing flux of hydrogen through the iron membrane in presence of O<sub>2</sub> is not yet fully understood. It could be interpreted as an effect of corrosion products which blocks the iron membrane surface. It may be emphasized that the quantity of precipitates, as determined by visual observations, was significantly higher for the test in presence of O<sub>2</sub>. However, it must be noted that tests with O<sub>2</sub> also resulted in doubling the corrosion rate. If a global blocking effect was at the origin of the decrease of hydrogen permeation, it would be expected that a similar consequence on the corrosion rate would take place, however this has not been observed.

It is also accepted that hydrogen sulfide promotes hydrogen charging via sulfur adsorbates, so it is not excluded that when the solution contains oxygen, interactions between sulfur adsorbates and oxygen adsorbates may reduce the hydrogen charging efficiency.

## 4 Conclusion

The effect of oxygen traces on corrosion and hydrogen embrittlement of pure iron was studied in aqueous NaCl (35g/L) under 1 bar H<sub>2</sub>S at ambient temperature with and without O<sub>2</sub> content corresponding to 500 ppb (12 mbar).

It has been observed that in the presence of oxygen, it reacts with H<sub>2</sub>S and predominantly produces sulfate (dissolved) as well as elemental sulfur precipitation. Sulfite and thiosulfate are also detected, but at a much lower concentration than sulfate. The reaction paths lead to acidification of the test medium to a range of one pH unit after one month compared to an oxygen-free test.

As expected, corrosion is strongly accelerated in the presence of O<sub>2</sub>, with a factor of about 2 under given conditions. Differences are also observed in the morphology and homogeneity of corrosion deposits. In addition, in both cases (with and without O<sub>2</sub>), XRD analyzes show mackinawite as the majority compound.

It is also observed that the permeation current density decreases in the presence of oxygen, which is rather surprising given the decrease in pH which is also observed, and which should have an opposite effect on the permeation current as it is on the corrosion rate. These antagonistic effects are not yet fully understood, but it is most likely that, the presence of the oxygen or products of the H<sub>2</sub>S / O<sub>2</sub> reaction has an effect on the hydrogen entry efficiency in the steel.

In order to improve the understanding of oxygen effects on corrosion mechanisms and embrittlement of steels, it is proposed to carry out electrochemical impedance spectroscopy measurements on the entry face of the membrane. Some tests shall be carried at the same pH using buffer solution, to avoid acidification of test solution in presence of oxygen. It is also planned to test other H<sub>2</sub>S/O<sub>2</sub> ratios by lowering H<sub>2</sub>S content in the test medium.

## References

- [1] NACE international, *NACE TM0284-2016 Evaluation of pipeline and pressure vessel steel for resistance to hydrogen induced cracking*.
- [2] Y. Song, A. Palencsár, G. Svenningsen, J. Kvarekvål, T. Hemmingsen., *Corrosion* 68 (2012) 662–671.
- [3] J.L. Crolet, M. Pourbaix, A. Pourbaix. *Corrosion/91*. 10-15 March. Cincinnati, OH (USA). NACE International, 1991.
- [4] J. Kittel, F. Ropital, F. Grosjean, E. M. M. Sutter, B.Tribollet., *Corrosion Science* 66 (2013) 324–329.
- [5] J.L Crolet, M.R Bonis. *Corrosion 2001*. 11-16 March. Houston, TX (USA). NACE International, 2001.
- [6] J.L Crolet, M. R. Bonis. *Corrosion 2010*. 14-18 March. San Antonio, TX (USA). NACE International, 2010.
- [7] M.A.V Devanathan and Z. Stachurski, *J. Electrochem. Soc.* 111 (1962) 619–623.
- [8] P. Manolatos, M. Jerome and J. Galland., *Electrochimica Acta* 40 (1995) 867–871.
- [9] W. Sun., *Kinetics of iron carbonate and iron sulfide scale formation in CO<sub>2</sub>/H<sub>2</sub>S corrosion*. Thèse de doctorat, The Russ College of Engineering and Technology of Ohio University, 2006.
- [10] C. Plenneveaux, *Etude des risques de corrosion et de rupture différée des aciers en présence d'H<sub>2</sub>S dans les conditions d'exploration de pétrole et de gaz à haute pression et haute température*. Thèse de doctorat, Institut National des sciences appliquées de Lyon, 2012.
- [11] T. Zakroczymski, Z. Szklarska-Smialowska, M. Smialowski., *Materials and Corrosion* 27 (1976) 625–630.